

IV-tuning: Parameter-Efficient Transfer Learning for Infrared-Visible Tasks

Yaming Zhang¹ Chenqiang Gao^{1,2*} Fangcen Liu¹ Junjie Guo¹ Lan Wang³ Xinggan Peng⁴
Deyu Meng⁵

¹ Chongqing University of Posts and Telecommunications ² Sun Yat-sen University ³ Michigan State University
⁴ Nanyang Technological University ⁵ Xi'an Jiaotong University

{YummyZhang1989, liufc67, gjj893866738}@gmail.com, gaochq6@mail.sysu.edu.cn,
wanglan3@msu.edu, xinggan001@entu.edu.sg, dymeng@mail.xjtu.edu.cn

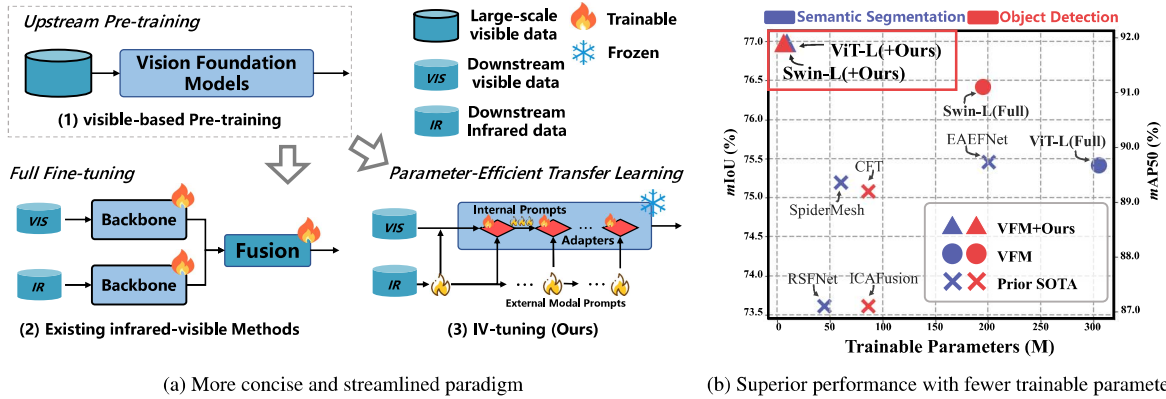


Figure 1. We demonstrate the superiority of the proposed method in both paradigm and performance, as illustrated. (a) (1): Vision Foundation Models (VFMs) are powerful pre-trained models that serve as robust backbones. (a) (1)→(2): Existing infrared-visible methods typically extend visible-based models into a dual-branch network and perform fine-tuning. (a) (1)→(3): We propose a more concise and streamlined framework for the parameter-efficient adaptation of visible-based VFMs to various infrared-visible tasks, including semantic segmentation and object detection. (b) Our proposed method achieves superior performance with fewer trainable parameters compared to previous state-of-the-art methods and VFMs.

Abstract

Infrared-visible (IR-VIS) tasks, such as semantic segmentation and object detection, greatly benefit from the advantage of combining infrared and visible modalities. To inherit the general representations of the Vision Foundation Models (VFMs), task-specific dual-branch networks are designed and fully fine-tuned on downstream datasets. Although effective, this manner lacks generality and is sub-optimal due to the scarcity of downstream infrared-visible datasets and limited transferability. In this paper, we propose a novel and general fine-tuning approach, namely “IV-tuning”, to parameter-efficiently harness VFMs for various infrared-visible downstream tasks. At its core, IV-tuning freezes pre-trained visible-based¹ VFMs and integrates modal-specific prompts with adapters within the

backbone, bridging the gap between VFMs and downstream infrared-visible tasks while simultaneously learning the complementarity between different modalities. By fine-tuning approximately 3% of the backbone parameters, IV-tuning outperforms full fine-tuning across various baselines in infrared-visible semantic segmentation and object detection, as well as previous state-of-the-art methods. Extensive experiments across various settings demonstrate that IV-tuning achieves superior performance with fewer training parameters, providing a good alternative to full fine-tuning and a novel method of extending visible-based models for infrared-visible tasks. The code is available at <https://github.com/Yummy198913/IV-tuning>.

¹Denotes training based on visible-modality data.

1. Introduction

In Computer Vision (CV), various tasks, such as semantic segmentation and object detection, have predominantly relied on the visible modality, and numerous visible-based methods [15, 45, 47, 56, 62] have spurred over the past decades. However, the performance of visible-based methods degrades in challenging scenarios (e.g., nighttime, fog, rain) due to the inherent limitations of visible imaging principles. Therefore, leveraging the infrared and visible images with strong complementary information to improve model performance has increasingly drawn attention. Various methods [11, 25, 33, 40, 57, 58] have been widely explored for the semantic segmentation or object detection with classic backbones, such as ResNet [12], VGGNet [43] and CSPDarkNet [1].

In recent years, Vision Foundation Models (VFMs), such as ViT [8], MAE [13], Swin Transformer [34] and DINOv2 [35] have demonstrated powerful generalization across various downstream tasks. Some infrared-visible methods [40, 57] have begun to leverage the general representations of VFMs to improve performance. As illustrated in Figure 1 (a) (1)→(2), these methods routinely introduce an additional infrared backbone branch with a structure identical to the visible branch. Subsequently, the entire model is fine-tuned on task-specific datasets. Albeit effective, they also expose some limitations: 1) *Complex fusion networks are designed task-specifically, which lack generalization.* 2) *Domain differences exist between infrared data and visible data used for pre-training [31]. Meanwhile, the commonly used infrared-visible datasets, such as MSRS [44] and M3FD [32], are significantly smaller than those used for pre-training VFMs, such as Imagenet [6] and LVD-142M [35]. When fine-tuning on limited datasets, the well-trained knowledge space of the VFMs could be disrupted [7, 37], resulting in inferior performance.* 3) *The full fine-tuning process is resource-intensive, time-consuming, and inefficient, particularly with dual-branch models, making it impractical for numerous applications and transfer deployments.* Hence, given the remarkable generalization of these VFMs across various downstream tasks, one intuitive question emerged: ***Can we harness the visible-based VFMs for infrared-visible tasks in a more efficient and general way?***

Parameter-Efficient Transfer Learning (PETL) methods are quickly introduced to Computer Vision due to their notable success in Natural Language Processing (NLP), such as prompt-tuning [17, 21, 36] and adapter-tuning [3, 24, 60]. By freezing the backbone and fine-tuning only a small portion of the parameters (less than 10% of the backbone), these methods demonstrate remarkable performance in various tasks. A more challenging task, however, is to simultaneously harmonize the efficient harness of inter-modal information and the adaptation of VFMs to downstream tasks.

In this work, we present *IV-tuning*, a novel and general

parameter-efficient transfer learning framework for adapting the visible-based Vision Foundation Models to downstream infrared-visible tasks, including infrared-visible semantic segmentation and object detection. As shown in Fig. 1 (a) (1)→(3), instead of adding an extra backbone branch for dual-modal learning, IV-tuning freezes the entire backbone of the VFMs and introduces infrared-specific prompts to the tuning process, which inherits the general representations of VFMs to the maximum extent. At its core, IV-tuning integrates modal prompts with adapters to function flexibly within the backbone, adapting VFMs to infrared-visible downstream tasks while simultaneously learning the complementarity between infrared and visible modalities. Specifically, the infrared modality information is utilized to generate modal-specific prompts with External Modal Prompt Generator (EMPG), avoiding the need for an extra network branch. Additionally, the Hybrid Adapter (HA) and the Internal Prompt Adapter (IPA) are inserted into each layer of backbones for further adaptation. The HA is used to optimize features from each frozen encoder layer, while the IPA enables IV-tuning to transform external modal prompts into internal ones, which interacts with the output of HA to jointly adjust the frozen backbone. This process effectively harmonizes the balance between upstream representations and downstream tasks, as well as the relationship between infrared and visible modalities. The main contributions of our work can be summarized below:

- We present IV-tuning, a novel and general framework for parameter-efficient fine-tuning infrared-visible tasks. Benefiting from learned modal prompts and adapters, the easily accessible VFMs can be effectively adapted to various infrared-visible tasks, including semantic segmentation and object detection.
- We propose the External Modal Prompt Generator, Hybrid Adapter, and Internal Prompt Adapter, which are used for valid modal prompts generation, visual features adaptation, and prompts transformation, respectively. The infrared modality information is streamlined into modal-specific prompts instead of introducing an additional network branch.
- Extensive experiments demonstrate the effectiveness of IV-tuning. By training approximately 3% of the parameters in backbones, IV-tuning achieves superior performance in infrared-visible semantic segmentation and object detection, outperforming the full fine-tuning paradigm and all the previous state-of-the-art methods, as shown in Fig. 1 (b).

2. Related Work

Vision Foundation Models. The Vision Foundation Models (VFMs) are pre-trained on large-scale datasets, e.g., ImageNet 21k [6], due to their ability to learn general representation, making them suitable for various downstream tasks.

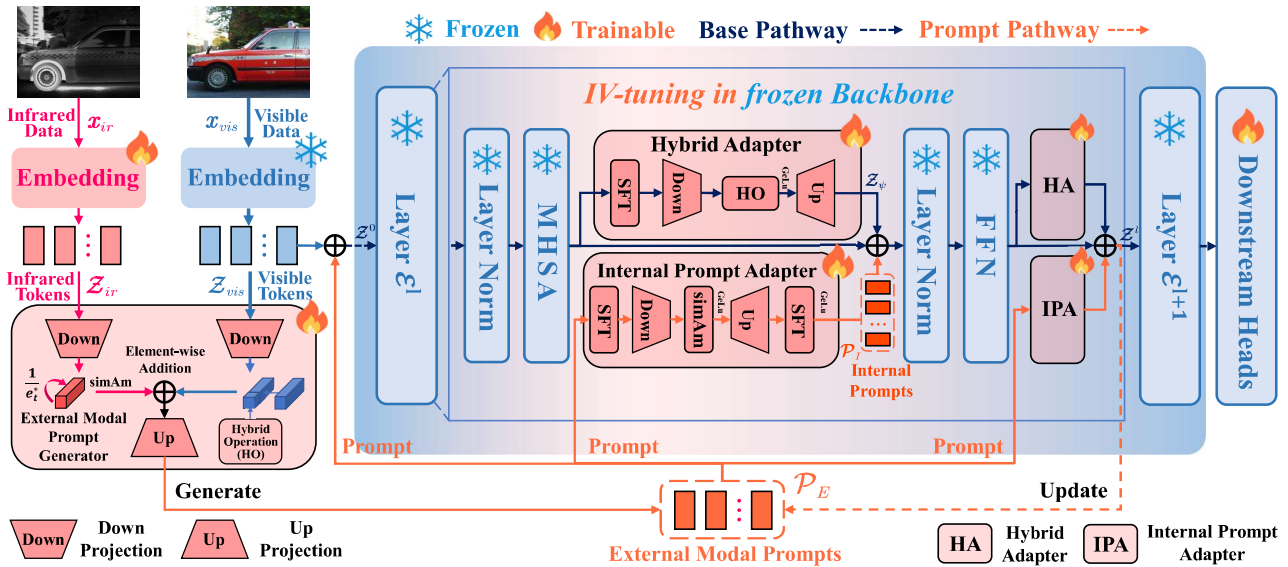


Figure 2. **The overview of the proposed IV-tuning.** IV-tuning freezes the L -layer transformer-based backbone and only fine-tunes a select few modules. The learned external modal prompts $\{\mathcal{P}_E^l\}_{l=1}^L$. The output of each encoder layer updates the external modal prompts. IV-tuning integrates adapter-tuning with prompt-tuning to collaboratively learn inter-modal complementarity while effectively adapting Vision Foundation Models to infrared-visible downstream tasks.

Many VFMs have emerged with the rise of Vision Transformers [8] in computer vision. For instance, with training on more than 400 million image-text pairs, CLIP [39] has demonstrated surprising performance in zero-shot classification tasks; MAE [14], which leveraged masked image modeling mechanism to learn representations in a self-supervised manner; and DINOv2 [35], which is pre-trained on a large, curated, and diverse dataset with discriminative self-supervision. These VFMs have shown strong generalization across various downstream tasks [30, 31, 46]. In this paper, we aim to explore harnessing VFMs to infrared-visible downstream tasks parameter-efficiently, leveraging their robust generalization capabilities for better performance.

Visual Parameters Efficient Transfer Learning. As more VFMs have emerged, efficiently adapting these large-scale pre-trained models to various downstream tasks has drawn much attention. To address the limitations of widely used full fine-tuning, Parameter-Efficient Transfer Learning (PETL) has emerged and serves as an excellent alternative to the full fine-tuning paradigm. In the computer vision community, Jia et al. [17] and Chen et al. [3] introduced prompt-tuning and adapter-tuning, respectively. Typically, these methods freeze the backbone and fine-tune only a few parameters. Prompt learning methods [17, 21, 36, 61] usually add some learnable parameters (i.e., prompts) into the input space, which helps the model remember pre-trained knowledge during fine-tuning. Adapter-tuning [3, 24, 51] inserts lightweight bottleneck

structures into the transformer encoder for adaptation. Both paradigms can achieve performance on par with or surpass that of the fully fine-tuning paradigm while reducing the training parameters significantly. However, existing methods mainly explore efficiently fine-tuning for one single task or are limited to one single modality [3, 17, 24, 36, 47, 61]. In contrast, we aim to extend the PETL paradigm to multiple infrared-visible scenarios, thus combining the respective advantages of dual-modal learning and efficient fine-tuning.

Recently, a study on unified infrared-visible downstream tasks was conducted [52], it introduced a Multi-modal Feature Pool (MFP) and a Supplementary Feature Injector (SFI) module, which operate in parallel with the ViT [8] model to incorporate dual-modality features into the ViT for infrared-visible tasks. In contrast, our method efficiently integrates prompt-tuning and adapter-tuning within a broader range of pre-trained foundational models, and explores the utility of PETL with a simpler design.

Infrared-visible Tasks. Infrared and visible are commonly used modalities with a natural complementarity. For advancing performance specifically in semantic segmentation or object detection, existing methods mainly adopt two approaches: (1) performing fusion at the image level, and feeding the fused image into semantic segmentation or object detection networks [19, 40, 57]. (2) designing end-to-end frameworks tailored for infrared-visible semantic segmentation or object detection [10, 11, 25, 26]. Whether training a designed network from scratch or fully fine-tuning a pre-trained model, these methods add an extra

backbone with a structure identical to the visible branch, where the infrared branch can only load visible-based parameters during fine-tuning. For example, CDDFuse [57] introduced a dual-branch Transformer-CNN feature extractor and performed a two-stage training method for semantic segmentation. Similarly, ICAFusion [40] utilized a dual-branch cross-attention transformer to enhance feature discriminability for objection detection. However, adding an extra branch network significantly increases model complexity and training consumption. Moreover, these methods are designed task-specifically, thereby limiting their generalization in different tasks. In this paper, we aim to propose a novel way of performing infrared-visible tasks, including semantic segmentation and object detection, achieving superior performance efficiently and generally.

3. Methodology

3.1. Overall Architecture

Compared to visible tasks, the infrared-visible tasks introduce an extra infrared input \mathbf{x}_{ir} , which is temporally synchronized and spatially aligned with the visible input \mathbf{x}_{vis} . These tasks aims to learn the mapping function F :

$$\mathbf{p} = F[\phi(f(\mathbf{x}_{vis}, \mathbf{x}_{ir}))], \quad (1)$$

where \mathbf{p} is the prediction result, ϕ is a task-oriented head, and f is a transformer-based Vision Foundation Model (VFM) (e.g., ViT [8] or Swin Transformer [34]) in our case. As shown in Fig. 2, we introduce an independent patch embedding layer for the infrared data, mapping the input image \mathbf{x}_{ir} to tokens of the same dimension D as the visible modality: $\mathcal{Z}_{ir} \in \mathbb{R}^{N \times D}$, where N is the token length. Then, the visible tokens \mathcal{Z}_{vis} and the infrared tokens \mathcal{Z}_{ir} are input to the External Modal Prompt Generator (EMPG) to generate external modal prompts \mathcal{P}_E , which are fused with the visible tokens in element-wise summation:

$$\mathcal{Z}^0 = \mathcal{Z}_{vis} + \mathcal{P}_E, \quad (2)$$

where \mathcal{Z}^0 is the prompted tokens that contain early-stage features from visible and infrared modalities, then it is injected into the first layer of a L -layer transformer encoder. Here we denote the \mathcal{Z}^{l-1} as inputs to the l -th encoder layer \mathcal{E}^l , and the \mathcal{Z}^l is the output of l -th encode layer \mathcal{E}^l , which is the external modal prompts for the next encoder layer. Formally, the process of the l -th encoder layer can be formulated as:

$$\mathcal{Z}^l = \mathcal{E}^l(\mathcal{Z}^{l-1}), \quad l = 1, 2, 3, \dots, L \quad (3)$$

$$\mathbf{p} = \phi(\mathcal{Z}^L), \quad (4)$$

where the transformer encoder layer \mathcal{E}^l includes Multi-head Self-Attention (MHSA), LayerNorm (LN), Feed-Forward Network (FFN).

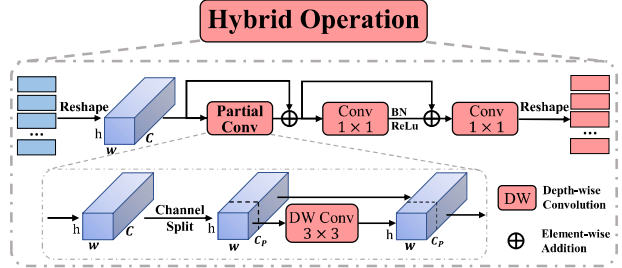


Figure 3. **Detailed design of our Hybrid Operation.** The input tokens are reshaped to feature maps, then a partial convolution is applied, followed by two 1×1 convolution layers with batch normalization and ReLU activation in between. We set the split channel C_P as $\frac{C}{4}$ by default.

Within each encoder layer, we insert the Hybrid Adapter (HA) ψ to enhance the transferability of VFMs. Specifically, given input features \mathcal{Z} from frozen layers, the adapted features \mathcal{Z}_ψ can be gained by:

$$\mathcal{Z}_\psi = \psi(\mathcal{Z}), \quad (5)$$

In the meantime, the external modal prompts \mathcal{P}_E are input to the Internal Prompt Adapter (IPA) for further feature transformation and adaptation, then generating internal prompts \mathcal{P}_I , which are added to adapted feature tokens in element-wise summation:

$$\mathcal{Z}_P = \mathcal{Z}_\psi + \mathcal{P}_I, \quad (6)$$

where \mathcal{Z}_P is the prompted internal tokens within the encoder layer. Note that we place two sets of {HA, IPA} modules after both the MHSA layer and FFN. The \mathcal{Z}_P obtained from the second {HA, IPA} module is then input to the next encoder layer of the VFMs.

3.2. External Modal Prompt Generator

In our case, a key challenge is not only to bridge the gap between upstream VFMs and downstream infrared-visible tasks, but also to explore the relationship between infrared and visible modalities. Existing prompt learning methods routinely prepend randomly initialized tokens that do not effectively align with the requirements of infrared-visible downstream tasks. Additionally, during inference, those prompts are static [60], limiting their ability to effectively correlate with information from any modality. To this end, we balance inter-modal learning alongside prompt learning. As illustrated in Fig. 2, EMPG receives the embedding tokens from both modalities $\{\mathcal{Z}_{vis}, \mathcal{Z}_{ir}\}$. The goal of EMPG is to learn modal prompts \mathcal{P}_E with infrared and visible data:

$$\mathcal{P}_E = EMPG(\mathcal{Z}_{vis}, \mathcal{Z}_{ir}), \quad (7)$$

Methods	CDDFuse [57]	CRM [41]	IGFNet [23]	RSFNet [25]	SpiderMesh [9]	EAEFNet [29]	SETR (baseline) [59]	+IV-tuning (Ours)	Segformer (baseline) [48]	+IV-tuning (Ours)
#TP	42.52M	50.70M	24.20M	44.53M	60.20M	200.40M	304.93M	8.90M (2.84%)	304.93M	8.90M (2.84%)
<i>mIoU</i>	64.30	69.78	73.53	73.61	75.20	75.46	75.08	75.51 (+0.43)	75.42	76.98 (+1.56)

Table 1. Overall performance on the MSRS dataset for infrared-visible semantic segmentation. The trainable parameters in backbones (#TP) and *mIoU* are reported.

Methods	CoCoNet [33]	TarDAL [32]	CBAM [5]	CDDFuse [57]	CFT [38]	ICAFusion [40]	CO-DETR (baseline) [62]	+IV-tuning (Ours)	DINO (baseline) [55]	+IV-tuning (Ours)
#TP	86.25M	86.25M	77.00M	86.25M	86.25M	86.25M	192.50M	6.06M (3.01%)	192.50M	6.06M (3.01%)
<i>mAP</i>	54.2	54.5	50.5	54.6	56.3	59.9	59.5	61.3 (+1.8)	60.2	61.1 (+0.9)
<i>mAP50</i>	80.7	80.9	81.0	81.1	87.1	89.2	90.2	90.6 (+0.4)	91.1	91.9 (+0.8)
<i>mAP75</i>	-	-	-	57.0	59.0	65.0	62.5	65.2 (+2.7)	64.1	66.0 (+1.9)

Table 2. Overall performance on the M3FD dataset for infrared-visible object detection. The trainable parameters in backbones (#TP), *mAP*, *mAP50* and *mAP75* are reported.

specifically, EMPG first projects infrared and visible data into lower-dimensional embeddings by:

$$\mathcal{M}'_{vis} \in \mathbb{R}^{N \times d_1} = s_1(\mathcal{Z}_{vis}), \quad (8)$$

$$\mathcal{M}'_{ir} \in \mathbb{R}^{N \times d_1} = s_2(\mathcal{Z}_{ir}), \quad (9)$$

where d_1 is the hidden dimension, $s_1(\cdot)$ and $s_2(\cdot)$ are 1×1 convolution layer. Concretely, considering that a single modal feature has redundancy, we propose the hybrid operation $g_h(\cdot)$ to process the visible tokens, as shown in Fig. 3. At the same time, we adopt simAM [49] to capture local spatial information across different channels in infrared images, which produces the enhanced embeddings \mathcal{M}'_{ir} by applying the channel-wise spatial attention weight $\frac{1}{e_t^*}$ over \mathcal{M}'_{ir} :

$$\mathcal{M}_{vis}^e = g_h(\mathcal{M}'_{vis}), \quad (10)$$

$$\mathcal{M}_{ir}^e = \mathcal{M}'_{ir} \odot \text{sigmoid}\left(\frac{1}{B}\right), \quad (11)$$

$$e_t^* = \frac{4(\delta^2 + \lambda)}{(t - \hat{\mu})^2 + 2\delta^2 + 2\lambda}, \quad (12)$$

where λ is a hyper parameter, t is input feature of a single channel, δ^2 and $\hat{\mu}$ are the energy factors calculated from input feature, B groups all e_t^* , and \odot is the Hadamard product. Lastly, we obtain mixed modal representations by additive binding, and the learned modal prompt can be gained by:

$$P_E = s_3(\mathcal{M}_{vis}^e + \mathcal{M}_{ir}^e), \quad (13)$$

where $s_3(\cdot)$ is the same as $s_1(\cdot)$ and $s_2(\cdot)$.

3.3. Hybrid Adapter

Adapters from NLP and CV [3, 16] typically conduct simple feature processing after down-projection, which is insufficient for images [50]. For balancing effectiveness and efficiency, we insert the proposed hybrid operation into

a standard adapter and introduce a simple feature transform strategy (SFT) to optimize task-agnostic representations from frozen encoder layers. Specifically, given input \mathcal{Z} from the frozen layers, the output \mathcal{Z}' of SFT is formulated as:

$$\mathcal{Z}' = LN(\mathcal{Z}) \odot \gamma + \beta, \quad (14)$$

where γ and β are learnable vectors, LN is the Layer-Norm. Formally, the output \mathcal{Z}_ψ of the Hybrid Adapter can be gained by:

$$\mathcal{Z}_\psi = [(GeLU(g_h(SFT(\mathcal{Z})\mathbf{W}_d^T)))\mathbf{W}_u^T] + \mathcal{Z}, \quad (15)$$

where the $\mathbf{W}_d \in \mathbb{R}^{r \times d_2}$ and $\mathbf{W}_u \in \mathbb{R}^{d_2 \times r}$ are the parameters of down-projection and up-projection, respectively, GeLU is the activation function.

3.4. Internal Prompt Adapter

Intrinsically, the external modal prompts \mathcal{P}_E contain low-level features from infrared and visible modalities, which can be reprocessed to benefit downstream tasks. However, features are highly nonlinearized after multi-layer encoder processing. We found that directly fusing the output of the Hybrid Adapter with external modal prompts \mathcal{P}_E causes performance degradation due to heterogeneous feature conflicts. To address this, we propose the Internal Prompt Adapter (IPA). As shown in Fig. 2, IPA operates on the external modal prompt \mathcal{P}_E , allowing the generated internal prompt \mathcal{P}_I to incorporate early-stage features. Note that existing methods [17, 60] usually compress the feature into a single token, constraining its ability to capture instance-level representations. In contrast, our IPA retains the complete modality information in the form of feature maps, prompting the model to fuse visible and infrared representations for better learning of inter-modal complementarities. Specifically, IPA is an adapter that contains two SFTs outside the bottleneck structure. In addition, after the

features are down projected to the d_3 dimension, we employ simAM [49] to enhance the features. Then, the internal prompts \mathcal{P}_I^l are obtained via a GeLU activation. The learned internal prompts are added to the output of Hybrid Adapter \mathcal{Z}_ψ^l to gain prompted tokens \mathcal{Z}_P^l as Eq. (6), which contains mixed blending representation. More details about the Internal Prompt Adapter are available in the supplementary material.

3.5. Optimization

During the tuning process, we freeze the parameters of VFMs and only optimize a few parameters $\theta = \{\tau^{ir}, \mathcal{P}_E, \{\mathcal{Z}_\psi^l\}_{l=1}^L, \{\mathcal{P}_I^l\}_{l=1}^L\}$, where τ^{ir} denotes the patch embedding layer of infrared inputs. Therefore, the optimization process can be formulated as:

$$\theta_{IV-tuning} = \arg \min_{\theta} \frac{1}{|\mathcal{D}|} \sum \mathcal{L}(\phi(\mathcal{Z}^L, \mathbf{y})), \quad (16)$$

where \mathcal{D} denotes the downstream infrared-visible data, \mathcal{L} denotes the overall loss function of IV-tuning, which is the same as that of the full fine-tuning model.

4. Experiment

4.1. Experiment Settings

IR-VIS Semantic Segmentation. MSRS [44] is a widely used dataset for infrared-visible semantic segmentation, which contains 1,444 pixel-annotated images with eight categories. The training and test sets have 1,083 and 361 image pairs, respectively. The evaluation metric employed is the mean Intersection over Union (*mIoU*). We compare our IV-tuning with state-of-the-art infrared-visible methods, including CDDFuse [57], CRM [41], IGFNet [23], RSFNet [25], SpiderMesh [9] and EAEFNet [29].

IR-VIS Object Detection. M3FD [32] is an infrared-visible object detection dataset containing 4,200 image pairs with six categories. The training and test sets have 3,360 and 840 image pairs, respectively. We report the *mAP*, *mAP50*, and *mAP75* to evaluate the performance comprehensively. We compare IV-tuning with state-of-the-art infrared-visible methods, including CoCoNet [33], TarDAL [32], CBAM [5], ICAFusion [40], CDDFuse [57] and CFT [38].

Vision Foundation Models. We employ ViT [8] and Swin Transformer (Swin) [34] as Vision Foundation Models (VFMs) for their representativeness as foundational architectures. To balance precision and efficiency, We employ the large version of these architectures. For semantic segmentation, we use ViT-L pre-trained on ImageNet-21k [6], and for object detection, we use Swin-L with COCO pre-trained parameters to ensure a fair comparison.

Implementation Details. We modify the mmsegmentation [4] and mmdetection [2] to support dual branch image input. We construct the baseline by full fine-tuning the entire

network. For semantic segmentation, we adopt the SETR [59] and Segformer [48] as segmentation heads to integrate with ViT-L. The SGD optimizer is employed with a learning rate of 1e-3. The experiments are configured to run for 160,000 iterations, and the images are cropped to 512×512 for a fair comparison. For object detection, we adopt CO-DETR [62] and DINO [55] as detection heads to integrate with Swin-L. The AdamW optimizer is employed with a learning rate of 1e-4. The model fine-tuning takes 36 epochs, and the images are cropped to 640×640 . We adopt identical experimental settings to the default full fine-tuning methods for each baseline. All experiments are conducted with a batch size of 2. By default, the hidden dimensions are set as follows: $d_1 = 8$ for EMPG, $d_2 = 64$ for HA, and $d_3 = 8$ for IPA, with the reason explained in the ablation study. Benefiting from streamlined architecture and reduced trainable parameters, IV-tuning can fine-tune models like ViT-Large or Swin-Large on a single RTX 3090, achieving superior performance with dual-modality input. Details regarding memory usage, storage, etc., are presented in the supplementary material.

4.2. IV-tuning on IR-VIS Semantic Segmentation

The experimental results of our IV-tuning on the MSRS dataset are presented in Tab. 1. Notably, our IV-tuning surpasses the full fine-tuning baselines, gaining an improvement of 0.57% and 2.06% with ViT-L+SETR and ViT-L+Segformer, respectively. This demonstrates that IV-tuning exhibits superior capability in adapting VFMs to downstream tasks. More discussion on the ‘‘adaptation’’ is available in the supplementary material. Besides, our IV-tuning beats all state-of-the-art methods, achieving the highest *mIoU* of **76.98%** and surpassing the best (EAEFNet [29]) by **2.01%**. Notably, some methods such as CDDFuse [57], ICAFusion [40] adopt a two-stage training while IV-tuning only fine-tuning less than **3%** of the backbone parameters in one single training stage, indicating that IV-tuning is highly competitive.

4.3. IV-tuning on IR-VIS Object Detection

As shown in Tab. 2, IV-tuning surpasses full fine-tuning in all baselines and outperforms previous state-of-the-art detectors while fine-tuning only **3.01%** of the parameters. In particular, IV-tuning achieves a **3%** improvement in *mAP* compared to the fully fine-tuning with Swin-L+CO-DETR. This indicates that our proposed IV-tuning still exhibits strong generalization in object detection tasks. Note that our IV-tuning also performs well with the Swin Transformer backbone, which is quite different from the ViT, (e.g., the feature scale and attention mechanism), indicating the effectiveness of our proposed approach.

4.4. Comparisons with other PETL Methods

To further explore the effectiveness of IV-tuning, we compare it with various Parameter-Efficient Transfer Learning (PETL) methods from both NLP (Adapter [16], prefix-tuning [27] and Bitfit [53]), and CV (VPT [17], AdaptFormer [3], Bi-AdaptFormer [20] and Rein [47]). We conduct experiments using ViT-L+Segformer for semantic segmentation and Swin-L+CO-DETR for object detection. We introduce the ‘‘Freeze’’ method to observe the effect of freezing the entire backbone without adding any new parameters, while only training the segmentation heads or detection heads. Note that we insert an independent infrared patch embedding layer in VFMs and add the infrared tokens to the visible tokens to get dual-modal results. We followed the best-performing settings for each method. As shown in Tab. 3 and Tab. 4, none of the existing methods surpass the baseline in infrared-visible semantic segmentation. These methods are not inherently designed for dense prediction tasks; their relatively simple adapter structures [3, 16] and compressed prompts [17, 20, 27] limit their ability to leverage visual signals. Moreover, they lack mechanisms for integrated learning with infrared modality. In contrast, IV-tuning enables more granular feature extraction and inter-modal interaction with hybrid adapters and modal prompts, resulting in improvements of **2.1%** and **3.0%** in *mIoU* and *mAP* compared to full fine-tuning. Furthermore, IV-tuning outperforms all PETL methods from NLP and CV in both semantic segmentation and object detection tasks, while remaining parameter-efficient. The comparisons between IV-tuning and UniRGB-IR [52] are presented in the supplementary material due to different experimental settings.

4.5. Ablation Study

We conduct ablation studies within two settings: ViT-L+Segformer for semantic segmentation and Swin-L+CO-DETR for object detection.

Analysis on each component. Our IV-tuning consists of three key components: the External Modal Prompt Generator, the Hybrid Adapter, and the Internal Prompt Adapter. As shown in Tab. 5 (a), when no components are included, we take the ‘‘Freeze’’ as a result, which only achieves a *mIoU* of 64.91% and a *mAP* of 56.6%, respectively. The EMPG brings performance gains of 12.2% to *mIoU*, and 6.7% to *mAP*, with only introducing 0.81M and 0.02M parameters, respectively. When the hybrid adapter is included, the performance increases to 76.53% of *mIoU* and 60.5% of *mAP*, respectively. We further combine the IPA with the HA to gain 76.98% and 61.3% performance, which brings 1.0% and 1.3% performance gains compared to no internal prompts, indicating the potential of internal prompts.

Analysis on the inserted layers. Reducing the number of inserted layers can significantly decrease the trainable parameters. As shown in Tab. 5 (b), we observe that the per-

Methods	Reference	#TP	<i>mIoU</i>	<i>mAcc.</i>
Segformer [48] (baseline)	NeurIPS 21	304.93M	75.42	83.43
Freeze	-	0.00M	64.91	72.14
<i>PETL Methods in NLP</i>				
+Adapter [16]	ICML 19	0.79M	32.98	37.49
+Prefix tuning [27]	ACL 21	0.91M	72.09	79.97
+BitFit [53]	ACL 21	1.06M	73.92	81.07
<i>PETL Methods in CV</i>				
+VPT-deep [17]	ECCV 22	1.96M	73.27	81.14
+AdaptFormer [3]	NeurIPS 22	3.96M	71.06	78.64
+Bi-AdaptFormer [20]	ICCV 23	2.36M	72.03	79.74
+Rein [47]	CVPR 24	5.83M	74.17	81.62
+IV-tuning (Ours)	-	8.90M	76.98	85.21

Table 3. Comparisons of Parameter-Efficient Transfer Learning (PETL) methods from NLP and 2D Vision on MSRS Datasets with ViT-L. The trainable parameters in backbones (#TP), *mIoU* and mean accuracy (*mAcc.*) are reported.

Methods	Reference	#TP	<i>mAP</i>	<i>mAP75</i>
CO-DETR [62] (baseline)	ICCV 23	192.50M	59.5	62.6
Freeze	-	0.00M	56.6	58.2
<i>PETL Methods in NLP</i>				
+Adapter [16]	ICML 19	4.67M	60.9	64.9
+Prefix tuning* [27]	ACL 21	0.10M	59.9	63.4
+BitFit [53]	ACL 21	0.52M	59.6	61.5
<i>PETL Methods in CV</i>				
+VPT-shallow* [17]	ECCV 22	0.05M	60.4	64.4
+AdaptFormer [3]	NeurIPS 22	2.34M	60.1	62.8
+Bi-AdaptFormer [20]	ICCV 23	1.16M	61.3	64.7
+Rein [47]	CVPR 24	14.72M	60.9	64.8
+IV-tuning (Ours)	-	6.01M	61.3	65.2

Table 4. Comparisons of Parameter-Efficient Transfer Learning (PETL) methods from NLP and 2D Vision on M3FD Datasets with Swin-L. The trainable parameters in backbones (#TP), *mAP* and *mAP75* are reported. Mark * denotes methods that can’t be fully migrated to Swin-L, and we do our best to tune them for optimal performance.

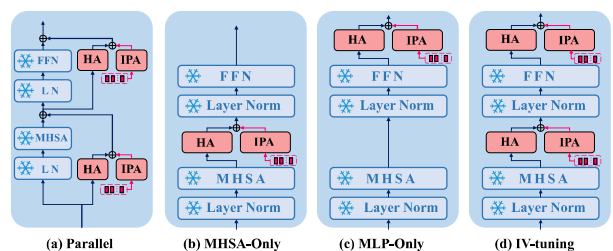


Figure 4. Variants of adapter-structure and IV-tuning.

formance of IV-tuning consistently improves as the number of inserted layers increases. Only fine-tuning on shallow or deep layers leads to different performance drop levels, indicating the necessity to fine-tune each frozen layer. Notably, when the parameters are reduced to 3.85M (see Tab. 5 (b) 1→9), IV-tuning can still beat all the state-of-the-art PETL methods while keeping the trainable parameters at a

EMPG	HA	IPA	MSRS		M3FD	
			#TP	<i>mIoU</i>	#TP	<i>mAP</i>
Full fine-tuning			304.93M	75.42	6.06M	61.1
Freeze			0.00M	64.91	0.00M	56.6
✓			0.81M	72.80	0.02M	60.4
✓	✓		7.77M	76.53	5.23M	60.5
✓	✓	✓	8.90M	76.98	6.06M	61.3

(a) Ablation study on each component.

Layers	MSRS	
	#TP	<i>mIoU</i>
1→9	3.85M	75.55
1→14	5.53M	76.48
1→19	7.21M	76.07
6→24	7.21M	76.70
1→24	8.90M	76.98

(b) Ablation study on inserted layers.

Settings	MSRS		M3FD	
	#TP	<i>mIoU</i>	#TP	<i>mAP</i>
Parallel	8.90M	50.61	6.06M	56.9
EMPG-Only	0.81M	72.80	0.02M	60.4
MHSA-Only	4.86M	76.28	3.04M	61.1
MLP-Only	4.86M	76.20	3.04M	61.3
IV-tuning	8.90M	76.98	6.06M	61.3

(c) Ablation study of various variants.

Table 5. Ablation studies on each component, inserted layers, and variants of IV-tuning, the trainable parameters in backbones (#TP), and the *mIoU* and *mAP* are reported.

EMPG	HA	IPA	#TP	<i>mIoU</i>	Δ_{8-64-8}
d_1	d_2	d_3			
8	16	8	3.79M (1.23%)	75.87	-1.44%
8	32	8	5.45M (1.76%)	76.06	-1.20%
8	64	8	8.90M (2.84%)	76.98	-
16	64	16	9.71M (3.09%)	76.92	-0.08%
32	64	32	11.33M (3.59%)	77.05	+0.09%

Table 6. Ablation studies on the hidden dimension of three modules. The trainable parameters in backbones (#TP), *mIoU*, and the performance changes relative to the “8-64-8” setting Δ_{8-64-8} are reported.

relatively low level.

Comparisons on the variants of IV-tuning. We create different variants (See Fig. 4), to investigate their impacts. As shown in Tab. 5 (c), when neither HA nor IPA is included (denoted “EMPG-only”), the performance only reaches 72.80% and 60.4%. We found that the “IV-tuning” setting achieves the best performance, potentially because placing an independent HA and IPA after MHSA and FFN layers allows for more flexible adaptation. Moreover, we found that the parallel style leads to significant performance drops, indicating that the sequential architecture is more effective than the parallel one.

Ablation on the hidden dimension. In IV-tuning, the three components all project the feature into lower dimensions, which is denoted by d_1 for EMPG, d_2 for HA, and d_3 for IPA. To explore their impact, we conduct a series of combinatorial experiments on the MSRS dataset. For simplicity, the hidden dimensions of EMPG and IPA are the same. As shown in Tab. 6, various parameter changes (3.79M → 11.33M) cause only slight performance changes, and the “8-64-8” parameter combination achieves an optimal trade-off between trainable parameters and performance, which is our default settings of IV-tuning.

More backbones. We evaluate the performance of IV-tuning with more backbones on the MSRS and M3FD datasets, respectively. For object detection with ViT [8], we employ ViTDet [28] due to the lack of available pre-trained weights for the large model. We present a complete comparison of different backbones in Tab. 7 and Tab. 8, IV-tuning outperforms the full fine-tuning paradigm across

multiple backbones in various downstream tasks with fewer trainable parameters, making it an excellent alternative to the full fine-tuning paradigm.

VFM-Head	Method	#TP	<i>mIoU</i>	<i>mAcc.</i>
ViT-L+Segformer	Full fine-tuning	304.93M	75.42	83.43
ViT-L+Segformer	Freeze	0.00M	64.91	72.14
ViT-L+Segformer	IV-tuning	8.90M (2.84%)	76.98	85.21
Swin-L+Segformer	Full fine-tuning	192.50M	78.23	85.74
Swin-L+Segformer	Freeze	0.00M	72.53	79.99
Swin-L+Segformer	IV-tuning	6.01M (3.03%)	78.60	85.83

Table 7. The performance of IV-tuning on ViT-L and Swin-L in the semantic segmentation task. The trainable parameters in backbones (#TP), the *mIoU*, and mean accuracy (*mAcc.*) are reported.

VFM-Head	Method	#TP	<i>mAP</i>	<i>mAP75</i>
Swin-L+CO-DETR	Full fine-tuning	192.50M	59.5	62.6
Swin-L+CO-DETR	Freeze	0.00M	56.6	58.2
Swin-L+CO-DETR	IV-tuning	6.06M (2.84%)	61.3	65.2
ViTDet-B	Full fine-tuning	85.89M	44.1	48.9
ViTDet-B	Freeze	0.00M	41.1	44.5
ViTDet-B	IV-tuning	3.66M (4.09%)	45.0	50.2

Table 8. The performance of IV-tuning on ViTDet-B (ViT-B) and Swin-L in the object detection task. The trainable parameters in backbones (#TP), the *mAP* and *mAP75* are reported.

5. Conclusion

In this work, we present IV-tuning, a novel parameter-efficient transfer learning framework for adapting visible-based Vision Foundation Models (VFMs) to infrared-visible tasks, including semantic segmentation and object detection. IV-tuning freezes the visible-based VFMs and introduces modal-specific prompts to the tuning process. By harmonizing prompt-tuning and adapter-tuning, we innovatively combine modal prompts with adapters to excavate the relationship between VFMs and infrared-visible downstream tasks, as well as the complementarity between the infrared and visible modalities. Extensive experiments demonstrate that IV-tuning is effective, efficient, and general in harnessing multiple VFMs across various downstream infrared-visible tasks.

IV-tuning: Parameter-Efficient Transfer Learning for Infrared-Visible Tasks

Supplementary Material

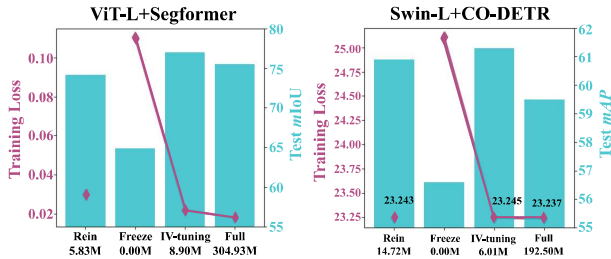


Figure 5. Training loss and test metrics on the MSRS [44] and M3FD [32] datasets, respectively. We use ViT-L [8] +Segformer [48] for semantic segmentation and Swin-L [34] +CO-DETR [62] for object detection, respectively. As the number of training parameters rises (Freeze \rightarrow IV-tuning \rightarrow Full), the training loss decreases. However, the metrics on the test set first rise and then fall, reaching a maximum at IV-tuning. This suggests that the full fine-tuning paradigm suffers from overfitting on the dataset, which provides strong evidence for the limitation of full fine-tuning stated in the main paper and further supports our motivation that **harnessing the VFMs parameter-efficiently for infrared-visible tasks yields superior performance**. Moreover, this phenomenon also applies to the comparison of Rein [47] and IV-tuning, suggesting that our IV-tuning better balances generalizability with the degree of training. The purple line denotes the average training loss when fine-tuned on the MSRS and M3FD datasets, respectively. The blue bars are the test metrics, including $mIoU$ and mAP , respectively.

6. Training Loss and Test Metrics

Overfitting has been a long-standing concern of researchers. Early neural network research [22] point out that as the training parameters increase, the models are prone to be “Overfitting”. The overfitted models tend to memorize all the data distribution, including the noise, instead of the discipline behind the data. This results in a loss of generalization on the test set.

In order to reduce the effect of overfitting, many solutions are proposed to inhibit the different triggers, such as the early-stopping, network-reduction and training data expansion. However, early stopping is still based on full fine-tuning, which imposes many limitations as mentioned in the main paper. Network pruning for large networks also greatly increases the difficulty of the practice, as it requires fine-tuning different parameters to observe performance changes. The complex acquisition conditions and strict labeling requirements also limit the expansion of dual-modal data. Hence, training with fewer parameters emerges as a feasible strategy for harnessing VFMs for infrared-

visible tasks.

In our main paper, numerous experiments have demonstrated the effectiveness of IV-tuning for adapting VFMs to downstream infrared-visible tasks. We hypothesize that the success of “adaptation” may be due to two factors: 1) *IV-tuning enhances the fitting capability of VFMs, allowing for better alignment with the training data.* 2) *IV-tuning reduces the overfitting of VFMs on small datasets, resulting in improved generalization during testing.* To investigate this, we calculate the average training loss of the last 1,000 iterations in semantic segmentation and that of the last 1 epoch in object detection, respectively, along with their corresponding evaluation metrics. As shown in Fig. 5, as the training parameters increase from Freeze (0.00M) \rightarrow IV-tuning (8.90M / 6.01M) \rightarrow Full fine-tuning (Full) (304.93M / 192.50M), the training loss monotonically decreases, suggesting that more trainable parameters can make the model better fit on the training set. However, the test metric increases and decreases, indicating that the full fine-tuning paradigm overfit on the training datasets. This observation aligns with the conclusion in Rein [47], providing strong evidence for the limitation of full fine-tuning discussed in our main paper and supporting our motivation that **harnessing the VFMs parameter-efficiently for infrared-visible tasks yields superior performance**. Moreover, this phenomenon also applies to the comparison of rein [47] and IV-tuning, indicating that our IV-tuning better balances generalizability with the degree of training.

7. Storage and Speed

Our proposed IV-tuning achieves superior performance by fine-tuning approximately 3% of the backbone parameters while significantly reducing training consumption. We present a comparison of training consumption for the experiments involving ViT-L [8] +Segformer [48] for semantic segmentation and Swin-L [34] +CO-DETR [62] for object detection, as discussed in the main paper. As shown in Tab. 9, compared to the full fine-tuning, IV-tuning reduces the training storage by **62.2%** and **51.9%** on the MSRS [44] and M3FD [32] datasets, respectively. IV-tuning also reduces the GPU memory by 17.1% and 2.4%, respectively. Specifically, for fine-tuning on N task-oriented datasets, IV-tuning only needs to store one set of the pre-trained parameters and N sets of the task-specific parameters, significantly reducing the training storage. We believe that as the size of pre-trained models gets larger, storage capacity will become a problem worth considering, whereas our IV-tuning presents a promising approach

Dataset	VFM-Head	Method	#TP	Storage	GPU Memory
MSRS	ViT-L+Segformer	Full fine-tuning	304.93M	3.7 GB	12.8 GB
	ViT-L+Segformer	IV-tuning	8.90M	1.4 GB	10.6 GB
M3FD	Swin-L+CO-DETR	Full fine-tuning	192.50M	2.7 GB	16.6 GB
	Swin-L+CO-DETR	IV-tuning	6.01M	1.3 GB	16.2 GB

Table 9. Comparison of trainable parameters in backbones (#TP), storage and GPU memory across multiple tasks.

Method	VFM	#TP	<i>mIoU</i>	<i>mAcc.</i>	Method	VFM	#TP	<i>mAP</i>	<i>mAP50</i>	<i>mAP75</i>	Method	VFM	#TP	<i>mAP</i>	<i>mAP50</i>	<i>mAP75</i>
UniRGB-IR	ViT-B	8.91M	82.80	94.30	UniRGB-IR	ViT-B	8.91M	44.1	81.4	40.2	UniRGB-IR	ViT-B	8.91M	63.2	96.1	72.2
IV-tuning	Swin-L	6.01M	86.86	92.59	IV-tuning	Swin-L	6.06M	45.8	83.2	42.9	IV-tuning	Swin-L	6.06M	66.7	96.9	77.8

(a) Comparison with UniRGB-IR on PST900 dataset.

(b) Comparison with UniRGB-IR on FLIR dataset.

(c) Comparison with UniRGB-IR on LLVIP dataset.

Table 10. Comparison with UniRGB-IR [52] on semantic segmentation and object detection tasks. We report the trainable parameters (#TP) in all experiments, with *mIoU*, mean accuracy (*mAcc.*) for semantic segmentation and *mAP*, *mAP50*, *mAP75* for object detection.

to solve it.

Algorithm 1 Internal Prompt Adapter.

```

# An example of Internal Prompt Adapter
import torch.nn as nn
import torch.nn.functional as F
import simAM
import SFT

class InternalPromptAdapter(nn.Module):
    def __init__(self, in_dim, hide_dim):
        super().__init__()
        self.norm = nn.LayerNorm(in_dim)
        self.down = nn.Linear(in_dim, hide_dim)
        self.up = nn.Linear(hide_dim, in_dim)
        self.act = nn.GELU()
        self.act_prompt = nn.GELU()
        self.simam = SimAM()
        self.sft1 = SFT()
        self.sft2 = SFT()

    def forward(self, x, hw_shapes):
        # Internal Prompt Adapter
        x = self.sft1(x)
        x = self.down(x)
        b, n, c = x.shape
        h, w = hw_shapes
        x = x.reshape(b, w, h, c).permute(0, 3, 1, 2)
        x = self.simam(x)
        x = self.act(x)
        x = x.permute(0, 2, 3, 1).reshape(b, n, c)
        x = self.up(x)
        x = self.sft2(x)
        # Generate Internal Prompts
        return self.act_prompt(x)

```

8. Comparisons with contemporaneous work

We demonstrate the comparison result of IV-tuning and UniRGB-IR [52] on semantic segmentation and object detection tasks, as shown in Tab. 10. Due to open-source issues, we present the performance results of IV-tuning on certain datasets mentioned in the UniRGB-IR. For the semantic segmentation on the PST900 [42] dataset, compared to UniRGB-IR, IV-tuning achieves the highest *mIoU* of 86.86%. For the object detection task on the FLIR [54]

dataset, IV-tuning brings performance gains of 3.9%, 2.2% and 6.7% in *mAP*, *mAP50* and *mAP75*, respectively. For the object detection task on the LLVIP [18] dataset, IV-tuning outperforms UniRGB-IR in all three test metrics. Notably, while achieving higher performance, IV-tuning fine-tunes a larger VFM (24 transformer encoder layers compared to 12 encoder layers) with fewer parameters (a reduction of 32.5%), clearly demonstrating its effectiveness and efficiency.

9. Algorithm of the Internal Prompt Adapter

Algorithm 1 describes the definition and computational procedure of our proposed Internal Prompt Adapter.

10. Visualization

In this section, we show the prediction results on the MSRS [44] and M3FD [32] datasets, including VFM-based full fine-tuning, Rein [47], and our IV-tuning. As shown in Fig. 6 and Fig. 7, under multiple comparative results, our method outperforms the other methods in terms of accuracy, demonstrating an effective improvement in the prediction of small objects and long objects while maintaining full attention on the large objects.

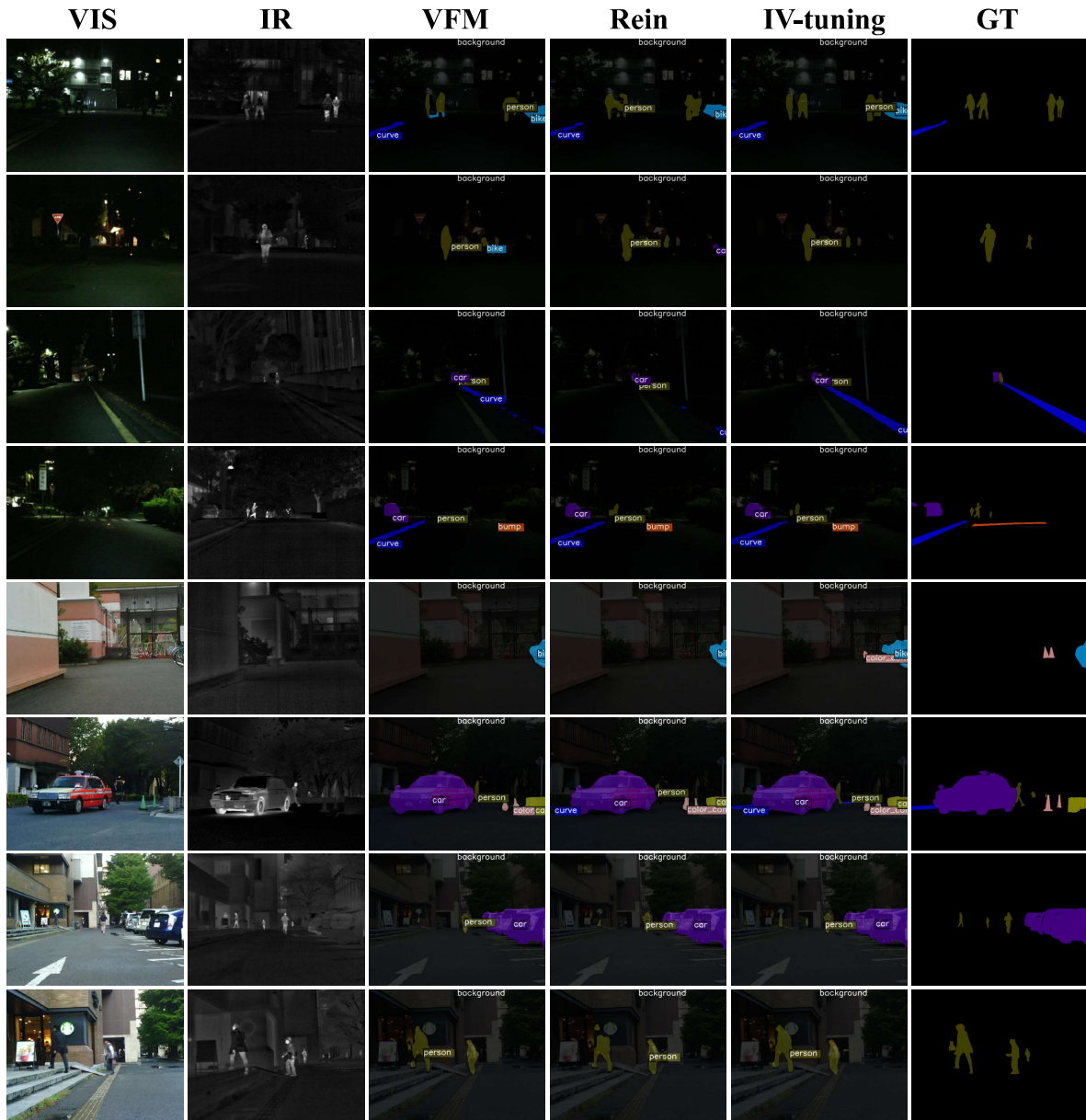


Figure 6. Prediction results of ViT-L+Segformer+IV-tuning on the MSRS dataset. We show a visual comparison with the Vision Foundation Model fully fine-tuned and Rein [47].

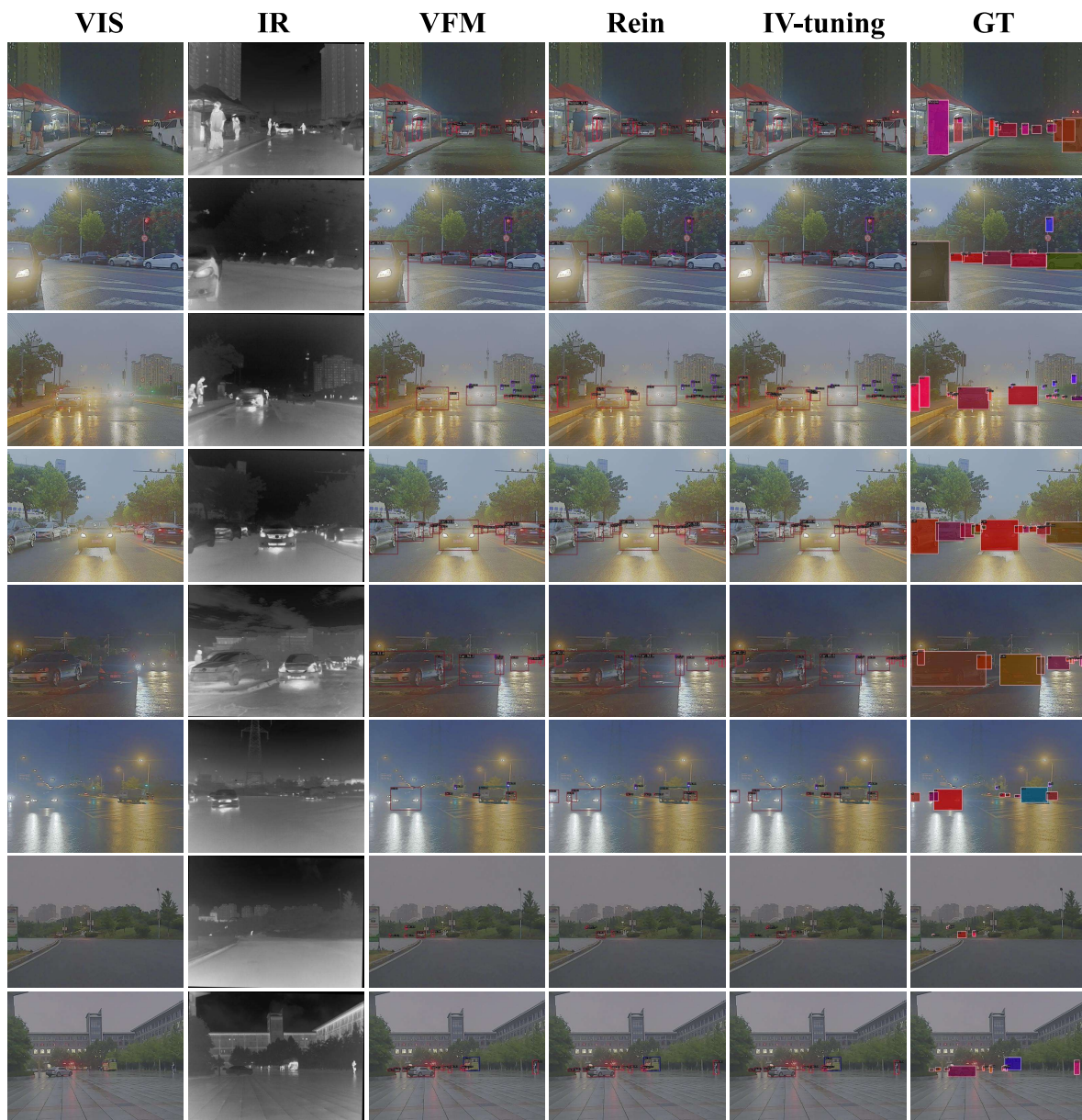


Figure 7. Prediction results of Swin-L+CO-DETR+IV-tuning on the M3FD dataset. We show a visual comparison with the Vision Foundation Model fully fine-tuned and Rein [47].

References

- [1] Alexey Bochkovskiy, Chien-Yao Wang, and Hong-Yuan Mark Liao. Yolov4: Optimal speed and accuracy of object detection. *arXiv preprint arXiv:2004.10934*, 2020.
- [2] Kai Chen, Jiaqi Wang, Jiangmiao Pang, Yuhang Cao, Yu Xiong, Xiaoxiao Li, Shuyang Sun, Wansen Feng, Ziwei Liu, Jiarui Xu, Zheng Zhang, Dazhi Cheng, Chenchen Zhu, Tianheng Cheng, Qijie Zhao, Buyu Li, Xin Lu, Rui Zhu, Yue Wu, Jifeng Dai, Jingdong Wang, Jianping Shi, Wanli Ouyang, Chen Change Loy, and Dahua Lin. MMDetection: Open mmlab detection toolbox and benchmark. *arXiv preprint arXiv:1906.07155*, 2019.
- [3] Shoufa Chen, Chongjian Ge, Zhan Tong, Jiangliu Wang, Yibing Song, Jue Wang, and Ping Luo. Adaptformer: Adapting vision transformers for scalable visual recognition. *Advances in Neural Information Processing Systems*, 35:16664–16678, 2022.
- [4] MMSegmentation Contributors. MMSegmentation: Openmmlab semantic segmentation toolbox and benchmark. <https://github.com/open-mmlab/mmdetection>, 2020.
- [5] Sri Aditya Deevi, Connor Lee, Lu Gan, Sushruth Nagesh, Gaurav Pandey, and Soon-Jo Chung. Rgb-x object detection via scene-specific fusion modules. In *Proceedings of the IEEE/CVF Winter Conference on Applications of Computer Vision*, pages 7366–7375, 2024.
- [6] Jia Deng, Wei Dong, Richard Socher, Li-Jia Li, Kai Li, and Li Fei-Fei. Imagenet: A large-scale hierarchical image database. In *2009 IEEE conference on computer vision and pattern recognition*, pages 248–255. Ieee, 2009.
- [7] Jesse Dodge, Gabriel Ilharco, Roy Schwartz, Ali Farhadi, Hannaneh Hajishirzi, and Noah Smith. Fine-tuning pre-trained language models: Weight initializations, data orders, and early stopping. *arXiv preprint arXiv:2002.06305*, 2020.
- [8] Alexey Dosovitskiy. An image is worth 16x16 words: Transformers for image recognition at scale. *arXiv preprint arXiv:2010.11929*, 2020.
- [9] Siqi Fan, Zhe Wang, Yan Wang, and Jingjing Liu. Spidernesh: Spatial-aware demand-guided recursive meshing for rgb-t semantic segmentation. *arXiv preprint arXiv:2303.08692*, 2023.
- [10] Zhen Feng, Yanning Guo, and Yuxiang Sun. Cekd: Cross-modal edge-privileged knowledge distillation for semantic scene understanding using only thermal images. *IEEE Robotics and Automation Letters*, 8(4):2205–2212, 2023.
- [11] Junjie Guo, Chenqiang Gao, Fangcen Liu, Deyu Meng, and Xinbo Gao. Damsdet: Dynamic adaptive multispectral detection transformer with competitive query selection and adaptive feature fusion. *ECCV*, 2024.
- [12] Kaiming He, Xiangyu Zhang, Shaoqing Ren, and Jian Sun. Deep residual learning for image recognition. In *Proceedings of the IEEE conference on computer vision and pattern recognition*, pages 770–778, 2016.
- [13] Kaiming He, Georgia Gkioxari, Piotr Dollár, and Ross Girshick. Mask r-cnn. In *Proceedings of the IEEE international conference on computer vision*, pages 2961–2969, 2017.
- [14] Kaiming He, Xinlei Chen, Saining Xie, Yanghao Li, Piotr Dollár, and Ross Girshick. Masked autoencoders are scalable vision learners. In *Proceedings of the IEEE/CVF conference on computer vision and pattern recognition*, pages 16000–16009, 2022.
- [15] Xiuquan Hou, Meiqin Liu, Senlin Zhang, Ping Wei, and Badong Chen. Saliency detr: Enhancing detection transformer with hierarchical saliency filtering refinement. In *Proceedings of the IEEE/CVF Conference on Computer Vision and Pattern Recognition*, pages 17574–17583, 2024.
- [16] Neil Houlsby, Andrei Giurgiu, Stanislaw Jastrzebski, Bruna Morrone, Quentin De Laroussilhe, Andrea Gesmundo, Mona Attariyan, and Sylvain Gelly. Parameter-efficient transfer learning for nlp. In *International conference on machine learning*, pages 2790–2799. PMLR, 2019.
- [17] Menglin Jia, Luming Tang, Bor-Chun Chen, Claire Cardie, Serge Belongie, Bharath Hariharan, and Ser-Nam Lim. Visual prompt tuning. In *European Conference on Computer Vision*, pages 709–727. Springer, 2022.
- [18] Xinyu Jia, Chuang Zhu, Minzhen Li, Wenqi Tang, and Wenli Zhou. Llvip: A visible-infrared paired dataset for low-light vision. In *Proceedings of the IEEE/CVF International Conference on Computer Vision*, pages 3496–3504, 2021.
- [19] Lihua Jian, Songlei Xiong, Han Yan, Xiaoguang Niu, Shaowu Wu, and Di Zhang. Rethinking cross-attention for infrared and visible image fusion. *arXiv preprint arXiv:2401.11675*, 2024.
- [20] Shibo Jie, Haoqing Wang, and Zhi-Hong Deng. Revisiting the parameter efficiency of adapters from the perspective of precision redundancy. In *Proceedings of the IEEE/CVF International Conference on Computer Vision*, pages 17217–17226, 2023.
- [21] Muhammad Uzair Khattak, Hanoona Rasheed, Muhammad Maaz, Salman Khan, and Fahad Shabbaz Khan. Maple: Multi-modal prompt learning. In *Proceedings of the IEEE/CVF Conference on Computer Vision and Pattern Recognition*, pages 19113–19122, 2023.
- [22] Steve Lawrence, C Lee Giles, and Ah Chung Tsoi. Lessons in neural network training: Overfitting may be harder than expected. In *Aaai/iaai*, pages 540–545, 1997.
- [23] Haotian Li and Yuxiang Sun. Igfnet: Illumination-guided fusion network for semantic scene understanding using rgb-thermal images. In *2023 IEEE International Conference on Robotics and Biomimetics (ROBIO)*, pages 1–6. IEEE, 2023.
- [24] Minglei Li, Peng Ye, Yongqi Huang, Lin Zhang, Tao Chen, Tong He, Jiayuan Fan, and Wanli Ouyang. Adapter-x: A novel general parameter-efficient fine-tuning framework for vision. *arXiv preprint arXiv:2406.03051*, 2024.
- [25] Ping Li, Junjie Chen, Binbin Lin, and Xianghua Xu. Residual spatial fusion network for rgb-thermal semantic segmentation. *Neurocomputing*, 595:127913, 2024.
- [26] Qing Li, Changqing Zhang, Qinghua Hu, Pengfei Zhu, Huazhu Fu, and Lei Chen. Stabilizing multispectral pedestrian detection with evidential hybrid fusion. *IEEE Transactions on Circuits and Systems for Video Technology*, 2023.
- [27] Xiang Lisa Li and Percy Liang. Prefix-tuning: Optimizing continuous prompts for generation. *arXiv preprint arXiv:2101.00190*, 2021.

- [28] Yanghao Li, Hanzi Mao, Ross Girshick, and Kaiming He. Exploring plain vision transformer backbones for object detection. In *European conference on computer vision*, pages 280–296. Springer, 2022.
- [29] Mingjian Liang, Junjie Hu, Chenyu Bao, Hua Feng, Fuqin Deng, and Tin Lun Lam. Explicit attention-enhanced fusion for rgb-thermal perception tasks. *IEEE Robotics and Automation Letters*, 8(7):4060–4067, 2023.
- [30] Zhiqiu Lin, Samuel Yu, Zhiyi Kuang, Deepak Pathak, and Deva Ramanan. Multimodality helps unimodality: Cross-modal few-shot learning with multimodal models. In *Proceedings of the IEEE/CVF Conference on Computer Vision and Pattern Recognition*, pages 19325–19337, 2023.
- [31] Fangcen Liu, Chenqiang Gao, Yaming Zhang, Junjie Guo, Jinhao Wang, and Deyu Meng. Infmae: A foundation model in infrared modality. *ECCV*, 2024.
- [32] Jinyuan Liu, Xin Fan, Zhanbo Huang, Guanyao Wu, Risheng Liu, Wei Zhong, and Zhongxuan Luo. Target-aware dual adversarial learning and a multi-scenario multi-modality benchmark to fuse infrared and visible for object detection. In *Proceedings of the IEEE/CVF Conference on Computer Vision and Pattern Recognition*, pages 5802–5811, 2022.
- [33] Jinyuan Liu, Runjia Lin, Guanyao Wu, Risheng Liu, Zhongxuan Luo, and Xin Fan. Coconet: Coupled contrastive learning network with multi-level feature ensemble for multi-modality image fusion. *International Journal of Computer Vision*, pages 1–28, 2023.
- [34] Ze Liu, Yutong Lin, Yue Cao, Han Hu, Yixuan Wei, Zheng Zhang, Stephen Lin, and Baining Guo. Swin transformer: Hierarchical vision transformer using shifted windows. In *Proceedings of the IEEE/CVF international conference on computer vision*, pages 10012–10022, 2021.
- [35] Maxime Oquab, Timothée Darcet, Théo Moutakanni, Huy Vo, Marc Szafraniec, Vasil Khalidov, Pierre Fernandez, Daniel Haziza, Francisco Massa, Alaaeldin El-Nouby, et al. Dinov2: Learning robust visual features without supervision. *arXiv preprint arXiv:2304.07193*, 2023.
- [36] Wenjie Pei, Tongqi Xia, Fanglin Chen, Jinsong Li, Jiandong Tian, and Guangming Lu. Sa²vp: Spatially aligned-and-adapted visual prompt. In *Proceedings of the AAAI Conference on Artificial Intelligence*, pages 4450–4458, 2024.
- [37] Matthew E Peters, Sebastian Ruder, and Noah A Smith. To tune or not to tune? adapting pretrained representations to diverse tasks. *arXiv preprint arXiv:1903.05987*, 2019.
- [38] Fang Qingyun, Han Dapeng, and Wang Zhaokui. Cross-modality fusion transformer for multispectral object detection. *arXiv preprint arXiv:2111.00273*, 2021.
- [39] Alec Radford, Jong Wook Kim, Chris Hallacy, Aditya Ramesh, Gabriel Goh, Sandhini Agarwal, Girish Sastry, Amanda Askell, Pamela Mishkin, Jack Clark, et al. Learning transferable visual models from natural language supervision. In *International conference on machine learning*, pages 8748–8763. PMLR, 2021.
- [40] Jifeng Shen, Yifei Chen, Yue Liu, Xin Zuo, Heng Fan, and Wankou Yang. Icafusion: Iterative cross-attention guided feature fusion for multispectral object detection. *Pattern Recognition*, 145:109913, 2024.
- [41] Ukcheol Shin, Kyunghyun Lee, In So Kweon, and Jean Oh. Complementary random masking for rgb-thermal semantic segmentation. In *2024 IEEE International Conference on Robotics and Automation (ICRA)*, pages 11110–11117. IEEE, 2024.
- [42] Shreyas S Shivakumar, Neil Rodrigues, Alex Zhou, Ian D Miller, Vijay Kumar, and Camillo J Taylor. Pst900: Rgb-thermal calibration, dataset and segmentation network. In *2020 IEEE international conference on robotics and automation (ICRA)*, pages 9441–9447. IEEE, 2020.
- [43] Karen Simonyan and Andrew Zisserman. Very deep convolutional networks for large-scale image recognition. *arXiv preprint arXiv:1409.1556*, 2014.
- [44] Linfeng Tang, Jiteng Yuan, Hao Zhang, Xingyu Jiang, and Jiayi Ma. Piafusion: A progressive infrared and visible image fusion network based on illumination aware. *Information Fusion*, 2022.
- [45] Chien-Yao Wang, Alexey Bochkovskiy, and Hong-Yuan Mark Liao. Yolov7: Trainable bag-of-freebies sets new state-of-the-art for real-time object detectors. In *Proceedings of the IEEE/CVF conference on computer vision and pattern recognition*, pages 7464–7475, 2023.
- [46] Ziyu Wang, Yanjie Ze, Yifei Sun, Zhecheng Yuan, and Huazhe Xu. Generalizable visual reinforcement learning with segment anything model. *arXiv preprint arXiv:2312.17116*, 2023.
- [47] Zhixiang Wei, Lin Chen, Yi Jin, Xiaoxiao Ma, Tianle Liu, Pengyang Ling, Ben Wang, Huaian Chen, and Jinjin Zheng. Stronger fewer & superior: Harnessing vision foundation models for domain generalized semantic segmentation. In *Proceedings of the IEEE/CVF Conference on Computer Vision and Pattern Recognition*, pages 28619–28630, 2024.
- [48] Enze Xie, Wenhai Wang, Zhiding Yu, Anima Anandkumar, Jose M Alvarez, and Ping Luo. Segformer: Simple and efficient design for semantic segmentation with transformers. *Advances in neural information processing systems*, 34: 12077–12090, 2021.
- [49] Lingxiao Yang, Ru-Yuan Zhang, Lida Li, and Xiaohua Xie. Simam: A simple, parameter-free attention module for convolutional neural networks. In *International conference on machine learning*, pages 11863–11874. PMLR, 2021.
- [50] Dongshuo Yin, Leiyi Hu Bin Li, and Youqun Zhang. Adapter is all you need for tuning visual tasks. *arXiv preprint arXiv:2311.15010*, 2023.
- [51] Dongshuo Yin, Yiran Yang, Zhechao Wang, Hongfeng Yu, Kaiwen Wei, and Xian Sun. 1% vs 100%: Parameter-efficient low rank adapter for dense predictions. In *Proceedings of the IEEE/CVF Conference on Computer Vision and Pattern Recognition*, pages 20116–20126, 2023.
- [52] Maoxun Yuan, Bo Cui, Tianyi Zhao, and Xingxing Wei. Unirgb-ir: A unified framework for visible-infrared downstream tasks via adapter tuning. *arXiv preprint arXiv:2404.17360*, 2024.
- [53] Elad Ben Zaken, Shauli Ravfogel, and Yoav Goldberg. Bitfit: Simple parameter-efficient fine-tuning for transformer-based masked language-models. *arXiv preprint arXiv:2106.10199*, 2021.

- [54] Heng Zhang, Elisa Fromont, Sébastien Lefevre, and Bruno Avignon. Multispectral fusion for object detection with cyclic fuse-and-refine blocks. In *2020 IEEE International conference on image processing (ICIP)*, pages 276–280. IEEE, 2020.
- [55] Hao Zhang, Feng Li, Shilong Liu, Lei Zhang, Hang Su, Jun Zhu, Lionel M Ni, and Heung-Yeung Shum. Dino: Detr with improved denoising anchor boxes for end-to-end object detection. *arXiv preprint arXiv:2203.03605*, 2022.
- [56] Hao Zhang, Feng Li, Huaizhe Xu, Shijia Huang, Shilong Liu, Lionel M Ni, and Lei Zhang. Mp-former: Mask-piloted transformer for image segmentation. In *Proceedings of the IEEE/CVF Conference on Computer Vision and Pattern Recognition*, pages 18074–18083, 2023.
- [57] Zixiang Zhao, Haowen Bai, Jianshe Zhang, Yulun Zhang, Shuang Xu, Zudi Lin, Radu Timofte, and Luc Van Gool. Cddfuse: Correlation-driven dual-branch feature decomposition for multi-modality image fusion. In *Proceedings of the IEEE/CVF conference on computer vision and pattern recognition*, pages 5906–5916, 2023.
- [58] Zixiang Zhao, Haowen Bai, Jianshe Zhang, Yulun Zhang, Kai Zhang, Shuang Xu, Dongdong Chen, Radu Timofte, and Luc Van Gool. Equivariant multi-modality image fusion. In *Proceedings of the IEEE/CVF Conference on Computer Vision and Pattern Recognition*, pages 25912–25921, 2024.
- [59] Sixiao Zheng, Jiachen Lu, Hengshuang Zhao, Xiatian Zhu, Zekun Luo, Yabiao Wang, Yanwei Fu, Jianfeng Feng, Tao Xiang, Philip HS Torr, et al. Rethinking semantic segmentation from a sequence-to-sequence perspective with transformers. In *Proceedings of the IEEE/CVF conference on computer vision and pattern recognition*, pages 6881–6890, 2021.
- [60] Xin Zhou, Dingkan Liang, Wei Xu, Xingkui Zhu, Yihan Xu, Zhikang Zou, and Xiang Bai. Dynamic adapter meets prompt tuning: Parameter-efficient transfer learning for point cloud analysis. In *Proceedings of the IEEE/CVF Conference on Computer Vision and Pattern Recognition*, pages 14707–14717, 2024.
- [61] Jiawen Zhu, Simiao Lai, Xin Chen, Dong Wang, and Huchuan Lu. Visual prompt multi-modal tracking. In *Proceedings of the IEEE/CVF conference on computer vision and pattern recognition*, pages 9516–9526, 2023.
- [62] Zhuofan Zong, Guanglu Song, and Yu Liu. Detr with collaborative hybrid assignments training. In *Proceedings of the IEEE/CVF international conference on computer vision*, pages 6748–6758, 2023.